An Exploration of Wall Retrofit Best Practices

Therese Stovall, PE
Member ASHRAE

Thomas Petrie, PhD
Member ASHRAE

Jan Kosny, PhD
Member ASHRAE

Phillip Childs

Jerry Atchley

Kimberly Sissom

ABSTRACT

A series of experiments were performed to examine wall retrofit options including replacing the cladding, adding insulation under the cladding, and multiple sealing methods that can be used when installing replacement windows in well-built or loosely-built rough openings. These experiments included thermal measurements in a hot box and air-leakage measurements. The retrofit claddings considered included wood-lap siding, vinyl siding, and vinyl siding with an integrated and formed foam insulation. Retrofit insulations included expanded and extruded polystyrene and foil-faced polyisocyanurate in various thicknesses. Air sealing methods for replacement windows included traditional caulking, exterior trim variations, loose-fill fiberglass, low-expansion foam, self-expanding foam inserts, and specialty tape. Results were applied to a model to estimate whole-house energy impacts for multiple climates.

INTRODUCTION

Approximately $140 billion was spent on residential remodeling in 2003, and almost $14 billion of that amount was spent on retrofitting siding ($5 billion), windows and doors ($8 billion), and insulation ($1 billion), as shown in Figure 1. (Harvard University, 2005) Although research has shown that these remodeling jobs are seldom motivated by energy costs, they present an opportunity to improve the energy-efficiency of the home. (Russell, 2006)

Standard guidance is available to calculate the thermal resistance of a wood- or metal-framed wall, but previous work has shown that these calculations are less accurate when used for intricate wall structures. Given the complexities introduced by a typical siding retrofit, where the new materials are laid upon the old as shown in Figure 2, experimental measurements offer a better indication of the heat transfer changes. The experimental program described here covered wall siding retrofit methods, air leakage at window-wall joints, and the combined effect of a window/wall retrofit. The experimental data were then used with a computer model to estimate the total annual energy savings for several typical houses in multiple locations. More detailed information about these experiments and analysis, including extensive tables of results, can be found in the project report. (Stovall, Petrie, et al., 2006)

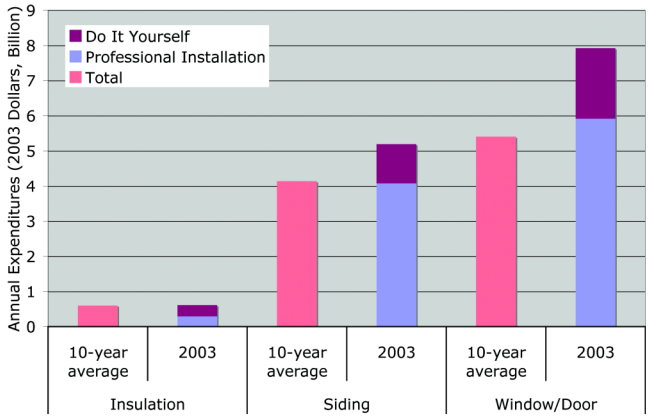

Figure 1 *Home improvement expenditures (source: Joint Center for Housing Studies of Harvard University).*

T.K. Stovall *is a senior research and development staff member,* ***T.W. Petrie*** *is a research engineer,* ***J. Kosny*** *is a senior staff scientist,* ***P.W. Childs*** *is a staff engineer, and* ***J.A. Atchley*** *is a research technician at the Building Envelopes Group, Engineering Science and Technology Division, Oak Ridge National Laboratory, Oak Ridge, TN.* ***K. Sissom*** *was a student at the University of Tennessee, Chattanooga.*

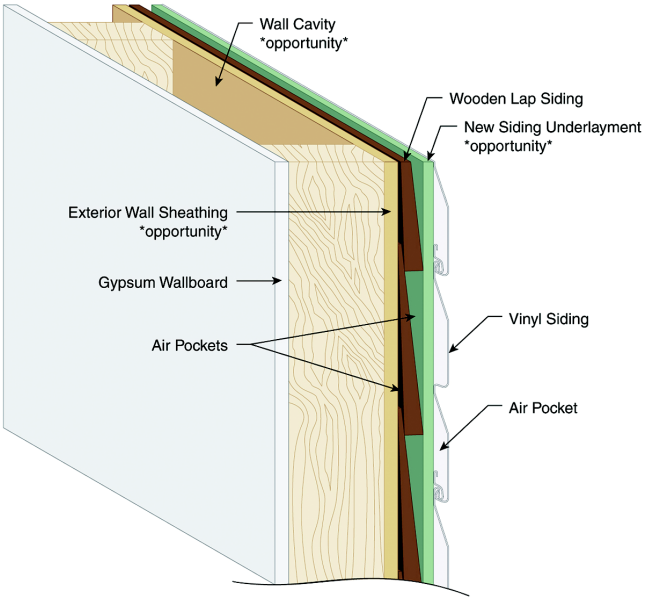

Figure 2 *Configuration when new siding is applied on top of existing wooden siding.*

Figure 3 *Wall framed to accept window, mounted in guarded hot box test frame.*

THERMAL PERFORMANCE TESTS

Apparatus and Test Conditions

The wall thermal measurements were made using a guarded hot box constructed and operated according to ASTM C 1363, *Standard Test Method for the Thermal Performance of Building Assemblies by Means of a Hot Box*. (ASTM, 2006) The metered section was 2.4 x 2.4 m (8 x 8 ft). The precision of this test method is reported to be approximately ±8%. All test results reported here have been corrected for guard energy losses, which ranged from 2.4% of the total measured heat flow for the most heavily insulated clear wall test to 0.7% for the least insulated wall with a window.

Each test ran from five to 11 days, as required to reach steady-state conditions, and the data results included in this report are average values taken over a time period ranging from 30 to 100 hours of steady-state operation. All tests were run with a mean climate-side temperature of 10°C (50°F) and a mean meter-side temperature of 38°C (100°F).

Specimen Preparation

The test walls were constructed to represent typical building practices, with 4 x 9 cm (nominal 2 x 4 in.) framing members placed on 40 cm (16 in.) centers, 1.3 cm (1/2 in.) gypsum wallboard screwed and taped on the metering side of the wall, and the cavity space between studs filled carefully with R-11 fiberglass batts. The wall's exterior sheathing was constructed of 1.3 cm (1/2 in.) plywood rather than the more common particleboard because this surface was subject to repeated fastenings as the siding was modified between tests. With this typical construction, 85.8% of the area is covered by insulated wall cavities, 10.5% by vertical studs, and 3.7% by horizontal tracks.

For the tests that included a window, the 0.9 x 1.2 m (3 x 4 ft) window was placed 86 cm (34 in.) from the bottom of the wall and along a stud 88 cm (35 in.) from one side wall. The window header was made of a sandwich of two 4 x 30 cm (nominal 2 x 12 in.) framing members with 1.3 cm (0.5 in.) plywood between them. The support below the window consisted of additional 4 x 9 cm (nominal 2x4 in.) framing members arranged as shown in Figure 3, which shows the wall frame installed in the guarded hot box test frame. Figure 4 shows this same wall after the cavity insulation and guard insulation have been added.

Thermocouple positions on the clear wall were maintained in the same location for all tests. The thermocouple positions were adjusted to provide more information around the window area for the window/wall combinations.

Smaller specimens, 60 x 60 cm (24 x 24 in.), taken from the insulation materials used in these tests were characterized independently using a heat flux meter apparatus operated in accordance with ASTM C 518. (ASTM, 2006) These tests were conducted at a mean temperature of 24°C (75°F) with a 22°C (40°F) temperature difference. (Stovall, Petrie, et al., 2006)

Six clear-wall configurations were tested, as shown in Table 1. All of these configurations were based on the same gypsum, frame, cavity insulation, and exterior plywood sheathing layers. Three of the structures used extruded polystyrene (XPS), one used polyisocyanurate, and one used expanded polystyrene (EPS). The left drawing in Figure 5 is

Table 1. Experimental Clear Wall Configurations

Base Case	Cedar lap siding
Mod 1	Cedar lap siding, 0.375 in. (1 cm) unfaced fan-fold XPS, vinyl siding
Mod 2	Cedar lap siding, 0.375 in. (1 cm) foil-faced fan-fold XPS, vinyl siding
Mod 3	Cedar lap siding, 0.5 in. (1.3 cm) unfaced XPS sheet, vinyl siding
Mod 4	Cedar lap siding, two layers of 0.5 in. (1.3 cm) foil-faced polyisocyanurate, vinyl siding
Mod 5	Cedar lap siding, EPS contoured foam-backed vinyl siding

Figure 4 *Wall frame after insulation placed in cavity and guard insulation added.*

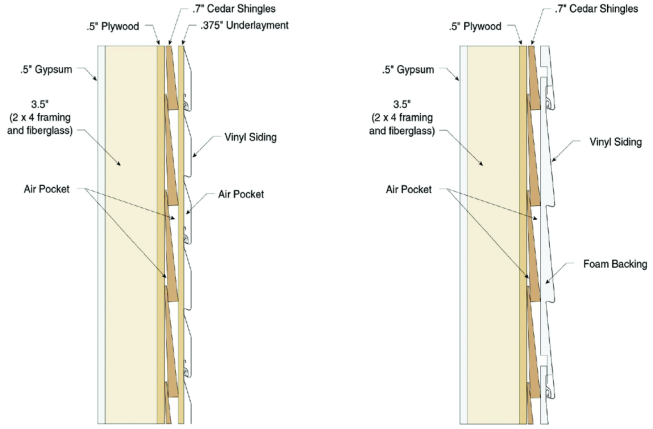

Figure 5 *Side views of retrofit vinyl siding configurations.*

representative of modifications 1-4, and the right drawing shows modification 5 (referred to throughout the rest of this paper as Mods 1-5).

The windows used for this experimental program were previously tested at the Mobile Window Thermal Test Facility (MoWiTT) and are described fully by Klems and Kelly (2003). These earlier tests provided an excellent characterization of the windows' seasonal performance. The flanged window, typical of many vinyl replacement windows, was tested with all six of the wall configurations listed in Table 1. A close-up look at the corner details on this window frame are shown in Figure 6. The unflanged (or insert) wood-framed, single paned window was tested in the Base Case wall, the Mod 2 wall, and the Mod 5 wall. This same single-pane window was re-tested in these same three configurations after the addition of an exterior low-e storm window.

Thermal Test Results

The thermal resistance of most wall systems tested in the guarded hot box can be determined by using weighted average surface temperatures that take into account the location and surface area of each component. That method applies for the six clear wall tests in this program. For the window/wall test specimens, however, it would not be meaningful to use a weighted surface temperature because the heat transfer mechanisms are complex, encompassing not only a wide difference in material properties, but also radiation heat transfer through the glass and non-uniform surface heat transfer coefficients. Therefore, only the air-to-air thermal resistance is relevant for these specimens.

Figure 7 compares the increase in thermal resistance of the wall retrofits to the thermal resistance of the products used to support the new vinyl siding. For the clear walls, the R-value increases slightly more than the insulation itself for most cases. The difference for Mod 1 should reflect the additional thermal resistance of the air space on each side of the underlayment, as well as that of the vinyl itself. This incremental resistance from the air spaces and vinyl should be approximately the same for Mods 1-4. The thermal resistance effect of the foil facing on the insulative underlayment can be determined by comparing the change in the clear wall R-value for Mods 1 and 2. The value of this reflective surface will, of course, vary according to the temperature difference across the space, but it provides ~ R-0.5 at the conditions tested here. As you go to the thicker insulation, Mods 3 and 4, the relative importance of the vinyl and trapped air space is reduced. For Mod 4, the greater thermal resistance of the underlayment

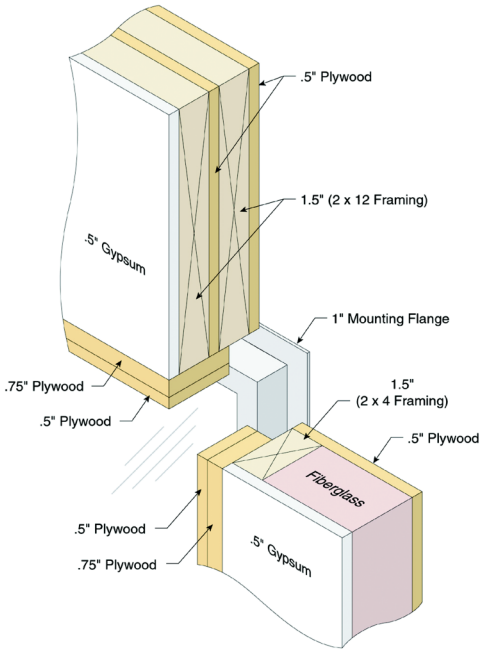

Figure 6 *Corner details for the flanged vinyl replacement window.*

material causes an increase in the temperature difference across the underlayment, thus increasing the average temperature within the fiberglass and within the underlayment itself. This will cause a very small decrease in the thermal resistance of both those materials. The insulation in Mod 5 is form-fitted to the vinyl siding, i.e., the insulation thickness varies from 1 to 2.5 cm (3/8 in. to 1 in.), so no direct comparison with the material itself can be made. There are no air spaces behind the vinyl with this product, but there would still be small air pockets between the cedar siding and the back of the insulation.

The change in overall wall R-value for the walls with a window is less than that of the clear walls because the major heat transfer path in this wall is the window itself. As shown in Figure 8, however, the energy savings in the wall with a window are about the same magnitude as those measured in the clear wall, even though the insulation now covers 19% less area.

The long-term window U-factors previously measured indicate that the performance of the single-paned window with the addition of a low-e storm window is almost as good as that of a replacement vinyl-framed double-paned window. (Klems and Kelly, 2003) The guarded hot box window-wall tests produced similar results. The energy consumption for these two options agreed to within 4%, and both showed about 40% less overall heat transfer than the wall containing the single-paned window, as shown in Figure 9. This relationship held true for all the wall treatments tested.

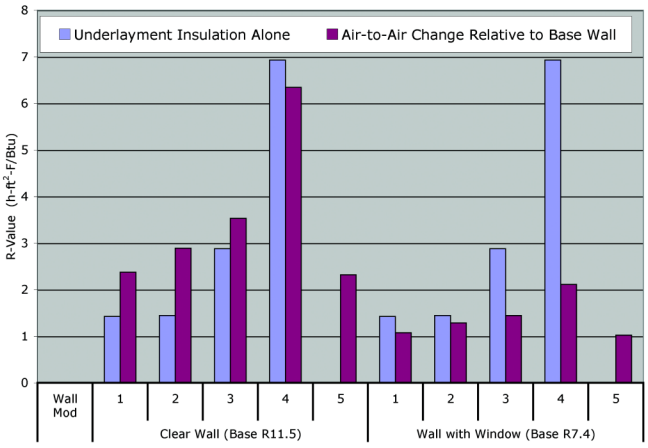

Figure 7 *Insulation R-values compared to wall air-to-air R-values.*

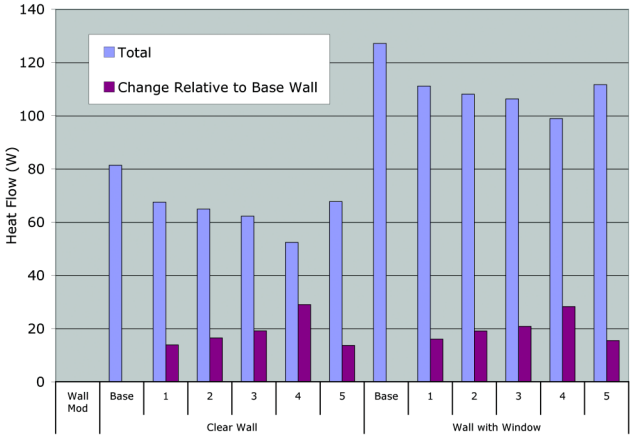

Figure 8 *Heat flow measured through wall sections in the guarded hot box.*

AIR LEAKAGE TESTS

It is challenging to characterize the air leakage associated with a window retrofit job because there is such a wide variation in window size, relative to rough opening size, and workmanship. Multiple metrics can be used to quantify air leakage, all based upon approximate relationships between air leakage and pressure drop. In buildings, air leakage is typically measured by using a blower door apparatus to pressurize the building and measure the air flow rate as a function of pressure difference. These data are typically fit to a power law curve of the form shown in Eq. 1.

$$Q = Co \times P^n \quad (1)$$

where:

Q = airflow rate,

Co = coefficient resulting from the curve fit,

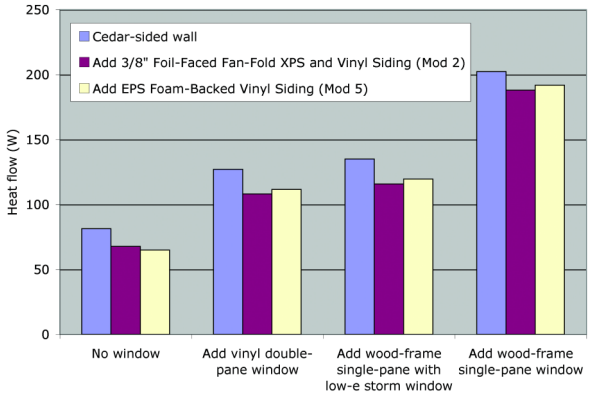

Figure 9 *Heat flow measured through window-wall sections in the RGHB.*

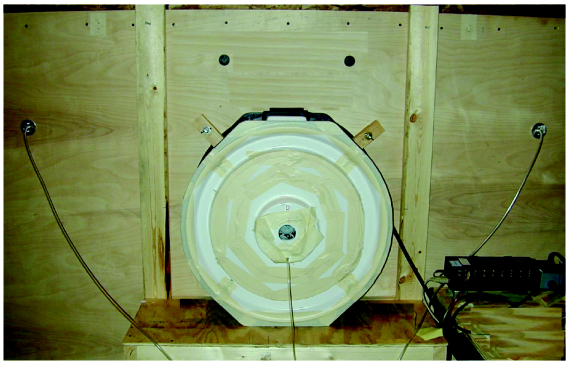

Figure 10 *Drilled holes in a plywood panel above fan opening to increase total airflow into the equipment's measurable range.*

P = applied pressure differential, and

n = exponent resulting from the curve fit.

Using this equation, it is common to quote the air leakage rates at pressure differences of 50 and 75 Pa. Another approximate relationship is used to express the same information in the form of the Estimated Leakage Area (ELA). The ELA is traditionally based upon an extrapolation of the data used for the curve fit in Eq. 1 to calculate the leakage flow rate at a pressure differential of either 10 Pa (Canadian "EqLA") or 4 Pa (LBNL "ELA"). (Sherman and Grimsrun, 1980a and 1980b) These air leakage values may be given on a per window basis, on an areal basis, or on a linear basis (where area here refers to the window opening area and the linear basis refers to the length of the window perimeter).

Development of the Test Apparatus

A new test apparatus was designed to take measurements in a geometry representative of a typical retrofit window. The air leakage tests were not directed toward measuring the air leakage of the window units, but rather that of the wall and of the wall/window interface. These tests were made using the approach described in ASTM E 283, *Standard Test Method for Determining Rate of Air Leakage Through Exterior Windows, Curtain Walls and Doors Under Specified Pressure Differences Across the Specimen*. (ASTM, 2006) In order to remove window assembly leakage from the measurements, all internal window joints were covered with tape. For some of the tests, the window unit was also covered with a plastic sheet.

A well-sealed box was affixed to the face of the same retrofit wall assembly used for the thermal tests. This box was leak-tested before each series of experiments. A Model 3 Minneapolis Blower Door Fan manufactured by the Energy Conservatory was mounted in a 1.3 cm (0.5 in) plywood panel constructed to adapt the blower door to the leak-tight enclosure, as shown in Figure 10. This plywood panel included a gasket and clamps to seal the fan to the surface of the wood and two small diameter holes, drilled about 61 cm (2 ft.) from the fan opening, to accommodate static pressure probes used to measure the pressure inside the enclosure.

The leakage through the retrofit wall proved to be below the measurable range of the system. Therefore, two holes were drilled in the plywood panel above the fan opening to increase the total air flow into the equipment's measurable range, as shown in Figure 10. This modified apparatus, including the chamfered holes, was calibrated by using a separate wall specimen known to have a leakage rate in the equipment's usual measurable range. (Stovall and Petrie et al., 2006) Based on a replicate series of measurements, the flow through both holes open with no other air leakage was characterized as

$$Q = 2.016\ P^{0.530} \qquad (2)$$

where

Q = ft^3/min and

ΔP = Pa

(or an LBNL Estimated Leakage Area of 7.69 cm^2(1.19 in^2)). The flow through each test specimen was then calculated as the difference between the measured result for that specimen and the known flow through the chamfered holes in the apparatus.

Air Leakage Error Analysis

Because this apparatus was specially designed to measure very low leakage rates, careful attention was given to a system-wide error analysis. All the air-leakage results reported here include the uncertainty bounds at a 95% confidence level.

The software provided by the blower door manufacturer was used to gather a large number of data points for each measurement, reducing the measurement uncertainty. (Energy Conservatory, 2006) The software reports precisions from ±0.1% to ±0.4% for air flow rates between 4.7 and 14.2 l/s (10

and 30 cfm) at 50 Pa. Similarly, the data collection and analysis software calculates the precision of the LBNL and Canadian leakage areas. These values are 6 to 10 times larger than the reported precisions for the leakage flow rates at 50 Pa, which makes sense because they are extrapolated to 4 Pa and 10 Pa, respectively, from the measured leakage curve.

The word *precision* is used to represent multiple statistical concepts. Here, we assumed that the reported precision corresponds to the measurement standard deviation, or standard deviation of the mean and confirmed this interpretation by checking the values observed during the evolution of the average of 200 readings recorded at each pressure difference. The estimated uncertainty at a 95% confidence level is then twice the average of the software-reported precision values divided by the square root of the number of replicated tests, as shown in Eq. 3.

$$U_{95} = \pm 2 \frac{S_{\bar{x}}}{\sqrt{n}} \quad (3)$$

where:

U_{95} = uncertainty at the 95% confidence level (for infinite degrees of freedom),

$S_{\bar{x}}$ = measurement standard deviation, or standard deviation of the mean (reported by the software as the 'precision' for each test), and

n = number of replicated tests.(Dieck, 1997)

The uncertainty for each test was also modified to account for the fact that the flow through the test specimen was the difference between the measured result for that specimen and the known flow through the chamfered holes in the apparatus. The uncertainty for a difference is the square root of the sum of the squares of the uncertainties of each component of the difference. (Dieck, 1997)

For most tests at 50 Pa, the final estimated uncertainty was well within the ±5% guideline of ASTM E 283. As a further test of the modified air leakage measurement technique, one window/wall configuration with an air leakage great enough to reach the range of the instrument without the use of the auxiliary holes was tested both directly and via the difference method. These two tests agreed to within 3%.

The absolute magnitude of the greatest uncertainty for all of these tests was no more than 7 times the smallest uncertainty. But the leakage rates themselves varied by a factor of more than 100. Therefore, on a relative basis, the tests with very small leakage rates will have a greater uncertainty, especially for the ELA. Figure 11 shows the raw data for three such low-leakage rate tests, along with the air flow through the calibrated holes from Eq. 2. For these three tests, the ELA varied from 0.0021 to 0044 in.^{2}/ft. (0.0044 cm^2/m to 00.93 cm^2/m). When the data from all three replicate tests are combined into a single data set, the ELA is calculated at 0.0030 in^2/ft. (0.0064 cm^2/m). For this set of replicate tests, the uncertainty was ±10% at 50 Pa and ±90% at 4Pa.

In summary, the procedure and apparatus that were used appear to be sensitive enough to discern very small differences in the air leakage due to the various methods used to seal the gap around the perimeter of the window.

Air Leakage Test Specimens

The base case wall with no window was the first configuration tested for air leakage. Because the critical air flow resistance was provided by the gypsum and plywood sheathing, air leakage tests were not repeated for the other siding materials.

As described previously, a vinyl flanged window and a wooden insert window were installed sequentially in the retrofit wall specimen. A storm window modification to the wooden insert window was also included in the thermal test schedule, but because the air leakage of interest here is that between the window and the wall framing, air leakage tests were not performed for that configuration.

A single test of the vinyl flanged window-wall combination was performed with the cedar lap siding in place. For this test, the exterior of the window frame was caulked directly to the siding. However, the window/wall joint was the subject of multiple modifications. To assure a repeatable and consistent condition on the wall exterior throughout the test schedule, the siding was removed and the bare plywood sheathing was used as the external wall surface for all the other air leakage tests.

Two different gap widths were tested, 1 and 1.9 cm (3/8 and 3/4 in.). Good building practice usually calls for the 1 cm spacing to allow for proper window alignment. The thicker gap was included in the test schedule to represent homes built with poor quality workmanship.

The window trim details were varied throughout the experimental program. These trim pieces included a brick molding trim placed on the exterior side of the wooden insert window frame, and flat pieces of plywood used to represent typical interior trim sizes and placement.

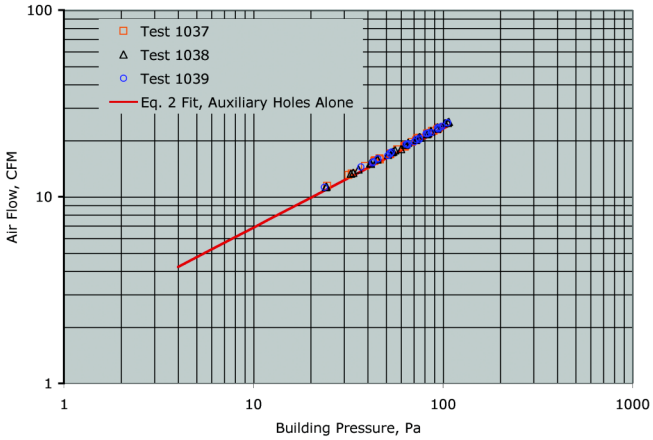

Figure 11 *Raw test data for three replicate low leakage rate tests.*

In addition to the varied window trim details, five gap treatments available to remodelers were tested:

- Loose fiberglass, commonly used to reduce air flow was stuffed into the gap. (Although good building practice calls for backer rod and caulking to be placed on top of the fiberglass, the fiberglass was tested independently here.)
- A bituminous tape product designed for this purpose was used to cover the joint between the window and the wall on the exterior side.
- A compressed foam tape was pre-applied to the side of the window frame before its placement in the wall. This tape then expanded to fill the gap after the window was in position.
- An aerosol foam sold for this application was blown into the gap and trimmed according to the product directions.
- An untreated open gap was included for comparison.

Air Leakage Test Results

The leakage for the retrofit base wall was measured to be 0.2±0.1 l/s (0.4 ± 0.2 ft^3/min.) at 50 Pa, or an ELA of 0.23 ±0.12 cm^2 (0.035 ± 0.018 $in.^2$). For the walls with windows, the leakage is, of course, much greater. Figure 12 is a summary of the results of the more traditional gap treatment methods. The caulking and trim around the window frame had a significant effect on the air leakage flowing through the gap between the rough opening and the window frame. These results indicate that the caulking was especially effective when applied at the interior wall frame interface. The results also demonstrate that fiberglass, while not eliminating air leakage, reduces it greatly.

The relative effectiveness of the other gap treatments used, without caulking, is displayed in Figures 13 and 14. As discussed previously, the 95% confidence uncertainty ranges are much broader for the ELA values than for the 50 Pa flow rates. Looking at the ELA values shown in Figure 13, the bituminous tape and the aerosol foam appear to have about the same effectiveness. Examination of these results shows that the presence of interior trim is less important in assuring the performance of the bituminous tape and aerosol foam products than it is for the fiberglass and compressed foam tape applications.

The ELA values measured varied from low levels of 0.2 to 0.4 cm^2/m^2 for sealing with aerosol foam, or caulked inside trim and fiberglass in the gap, or a bituminous tape on the outside of the gap. They reached a range of 2 to 3 cm^2/m^2 with very little sealing but at least some trim and caulking on the exterior surface. The totally open large gap with no trim or caulking produced an ELA of more than 20 cm^2/m^2, which should represent a worst case scenario.

For comparison, the *2001 ASHRAE Fundamentals* offered four entries for window framing: uncaulked masonry, caulked masonry, uncaulked wood and caulked wood.(ASHRAE, 2001) Each entry was assigned a best estimate, minimum and maximum ELA. Values of ELA for wood windows vary from 0.3 to 2.7 cm^2/m^2. This range matches very well with the results from the tests reported here. The ASHRAE best estimate for caulked windows is the same as their minimum. The best estimate for uncaulked windows is 1.7 cm^2/m^2, which is exactly what we achieved with the uncaulked full plywood "trim" for the larger gap size tested. The uncaulked inside trim for the insert window and the smaller gap size yielded the maximum 2.4 cm^2/m^2, even when exterior caulking was used. In summary, these test results are in general agreement with the ASHRAE suggested values and should lend support to their use.

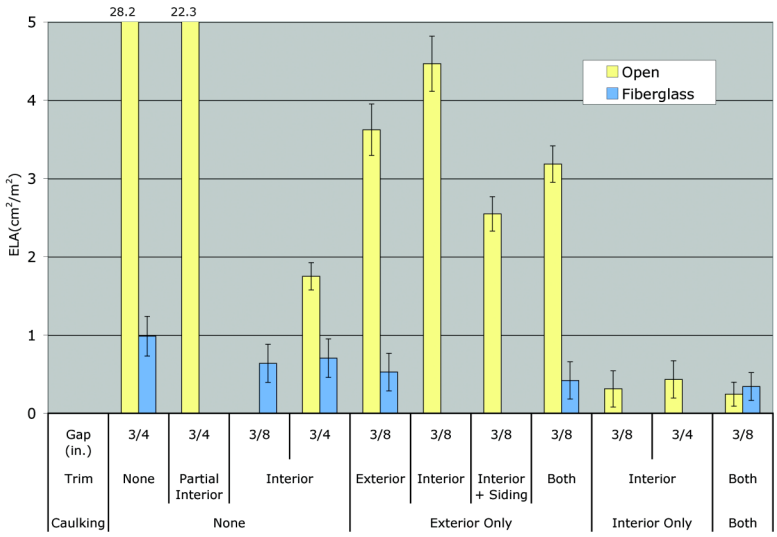

Figure 12 *Equivalent leakage area for open and fiberglass-stuffed window/wall joints for varying trim and caulking conditions, 95% confidence uncertainty limits shown.*

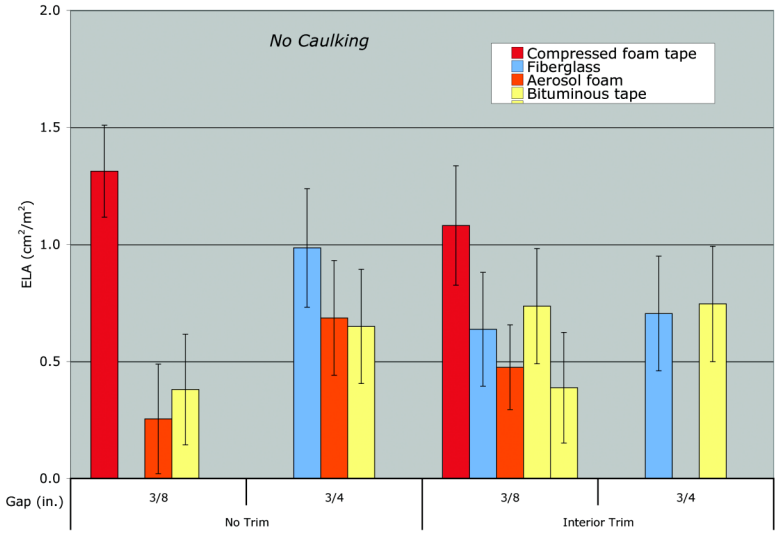

Figure 13 *Equivalent leakage area for a number of window/wall joint sealing products for two gap sizes, 95% confidence uncertainty limits shown.*

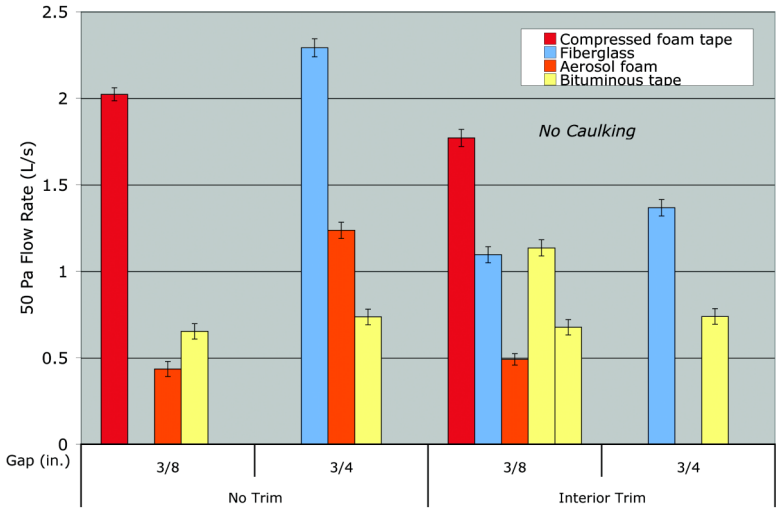

Figure 14 *Air leakage flow at a pressure difference of 50 Pa for a number of window/wall joint sealing products and two gap sizes, 95% confidence uncertainty limits shown.*

MODELING: WALL AND WINDOW RETROFITS

Our laboratory tests and those performed at LBNL established the thermal and infiltration characteristics of several common retrofit methods. These characteristics were used as input with whole house models to estimate the potential energy savings for multiple climates. Although these models include infiltration, these models do not address the effects of air-carried moisture deposition and the possible reduction in insulation value that can result from such moisture accumulation.

The measured R-values were used with whole house heating and cooling energy consumption correlations from a previous study of wall types and thermal characteristics using three house models in ten locations; see Figure 15.(Kosny et al., 2001 and Stovall, Petrie, et al., 2006) Two bases were used for these energy savings calculations, reflecting the two possible initial conditions. The first is an uninsulated wall and the second is an insulated wall. Table 2 summarizes these retrofit cases.

To consider the sum of heating and cooling energy savings, it was necessary to factor in the effect of heating and cooling system efficiencies and energy costs. Electricity and gas prices were taken from the Zip Code data base for each city. (Stovall, 2002 and Stovall, Petrie, et al., 2006) The air

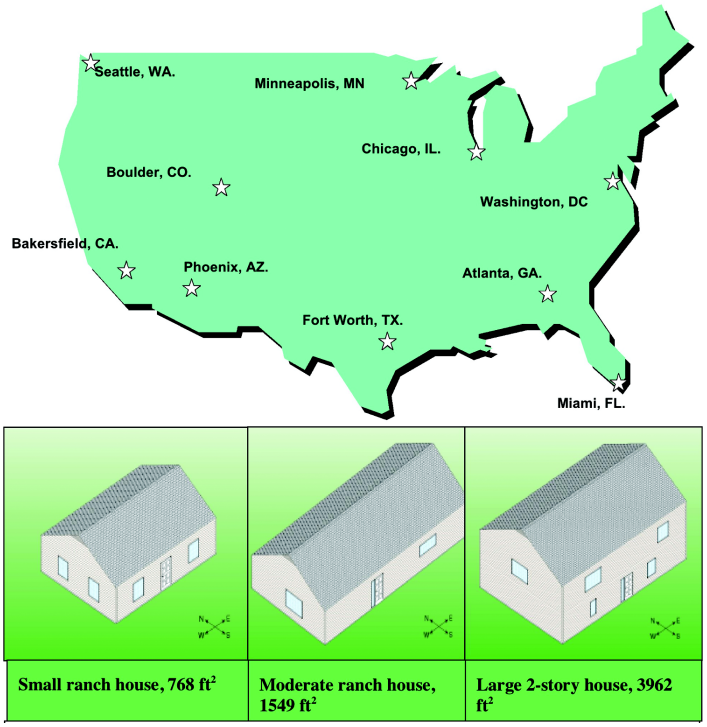

Figure 15 *Locations and house designs used for savings estimates.*

Table 2. Wall Retrofit Cases Considered for Energy Savings Model

Retrofit	Initial Condition	Final Condition
W1	Uninsulated wall cavity	Add R11batt cavity insulation and 0.375 in. fan-fold extruded polystyrene with vinyl siding (Mod 1 or 5)
W2	Insulated cavity	Add 0.375 in. fan-fold extruded polystyrene with vinyl siding (Mod 1 or 5)
W3	Insulated cavity	Add 0.375 in. fan-fold extruded polystyrene with foil facing with vinyl siding (Mod 2)
W4	Insulated cavity	Add 0.5 in.extruded polystyrene board with vinyl siding (Mod 3)
W5	Insulated cavity	Add 1 in. foil-faced polyisocyanurate foam with vinyl siding (Mod 4)

conditioner was assumed to have an SEER of 9 Btu/Wh and the gas furnace a seasonal efficiency of 80%. Duct losses were estimated at 20% for both seasons. The results, shown in Figure 16, demonstrate significant savings from 20 to 25% of total heating and cooling costs that occur if the homeowner elects to insulate a previously uninsulated wall during the retrofit process. The savings for adding up to 1-in. (2.5 cm) of foam insulation under new vinyl siding are over 10% for every city examined except for Miami. In Miami, a greater portion of the cooling load is latent, which is unaffected by improvements in the walls' thermal resistance.

These same three house models and locations were also used to examine the impact of the air-leakage reduction products tested. This modeling effort used the DOE2.1E code and the *ASHRAE Handbook* 'average' values for house component air leakage to place the retrofit window-wall gap reductions within the framework of the total house air leakage. (ASHRAE, 2001) The model predicts savings from 2 to 7% for the large two-story house, with lesser savings for the other two houses. Although the savings are modest, the cost of these measures is also small.

DISCUSSION

It was interesting to note that the energy savings from a wall cladding retrofit on a wall with a window were just as great as the savings for the same retrofit on a wall without a window, even though the treated area was 19% less. This is most likely attributable to the greater proportion of wall framing present in the wall with a window. External insulative sheathing is especially effective in reducing heat transfer through walls with greater framing heat transfer paths.

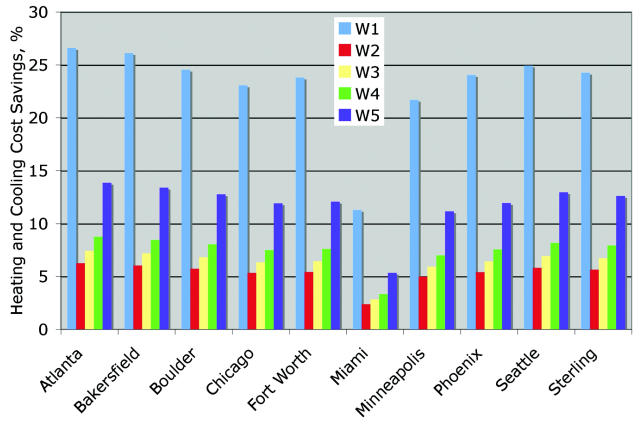

Figure 16 *Heating and cooling cost savings for ten cities for the small ranch house for five retrofit walls.*

Based on the air leakage measurements, the caulking and trim around a window frame, as well as the gap treatments used, have a significant effect on the air leakage flows. However, considering not only the variability in initial application quality, but also the variability in application status over time, employing redundant techniques to reduce air leakage around windows would be prudent.

The window framing air leakage experimental data reported here are comparable to those reported in the ASHRAE Handbook of Fundamentals volume that was current at the time these tests were made. (ASHRAE, 2001) However, that table has been deleted from the most recent *Fundamentals* volume. (ASHRAE, 2005) Researchers interested in this topic may want to hold on to the 2001 volume for reference.

CONCLUSIONS

Analysis has shown that homeowners are not motivated to retrofit their homes in order to reduce their utility costs. However, energy consumption can be reduced by taking some relatively simple extra steps during other retrofit projects, especially those involving walls and windows. Toward that end, an experimental program was implemented to measure the performance of a number of possible wall siding and window retrofit configurations, including thermal and air-leakage measurements. These results, combined with two analytical models, lead to annual utility cost savings estimates on the order of 10% for most locations. Additional savings are possible through the adoption of either low-e storm windows or replacement vinyl-framed double-paned windows.

REFERENCES

ASHRAE. 2001. *ASHRAE Handbook – Fundamentals*. Atlanta: American Society of Heating, Refrigerating, and Air Conditioning Engineers, Inc.

ASHRAE. 2005. *ASHRAE Handbook – Fundamentals*. Atlanta: American Society of Heating, Refrigerating, and Air Conditioning Engineers, Inc.

ASTM. 2006. ASTM International, PA.

Dieck, Ronald H. 1997. *Measurement uncertainty methods and applications*, 2d ed. The Instrumentation, Systems, and Automation Society. Research Triangle Park, NC.

Energy Conservatory. 2006. The Minneapolis Blower Door™. Minneapolis, MN. www.energyconservatory.com

Harvard University. 2005. The changing structure of the home remodeling industry: improving America's housing. Joint Center for Housing Studies of Harvard University.

Klems, J. and G. Kelly. 2003. Symposium paper KC-03-12-1, *ASHRAE Transactions* 109(2), June 28-July 2.

Kosny, J. and Desjarlais, A. O. 1994. Influence of architectural details on the overall thermal performance of residential wall systems. *Journal of Thermal Insulation and Building Envelopes*. Vol. 18, July.

Russell, B. 2006. The relationship between home energy costs and energy-related remodeling activity. N06-2, Joint Center for Housing Studies Harvard University, June.

Sherman, M.H. and D. T. Grimsrud. 1980(a). Infiltration-pressurization correlations: simplified physical modeling. *ASHRAE Transactions* 86 (2):778.

Sherman, M.H. and D. T. Grimsrud. 1980(b). Measurement of infiltration using fan pressurization and weather data. Air Infiltration Instrumentation and Measuring Techniques: 1st AIC Conference, October 6-8, Windsor Great Park, Berkshire, UK. pp 277-322.

T.K. Stovall. 2002. Supporting documentation for the 1997 revision to the Doe Insulation Fact Sheet, *ORNL-6907*, August.

Stovall, T. K. and T. W. Petrie, et al. 2006. An experimental and analytical evaluation of wall and window retrofit configurations: supporting the residential retrofit best practices guide. *ORNL/TM-165*. Oak Ridge National Laboratory, December 1.